LHCb-CONF-2011-035
15 July 2011

Analysis of $\overline{B}{}^0_s \to J/\psi\,(\pi^+\pi^-$ and $K^+K^-)$ and the first observation of $J/\psi f_2'(1525)$

The LHCb Collaboration[1]

Abstract

Measurement of mixing induced CP violation in $\overline{B}{}^0_s$ decays is of prime importance in probing new physics. So far only the channel $\overline{B}{}^0_s \to J/\psi\phi$ has been used. Here we investigate $\overline{B}{}^0_s$ decays into CP eigenstates and other modes in the $J/\psi\pi^+\pi^-$ and $J/\psi K^+K^-$ final states. The $\pi^+\pi^-$ mass spectrum has a relatively narrow structure peaking near 980 MeV first found by LHCb, that we identify as the $f_0(980)$, and show that it is consistent with being pure S-wave. Thus, this is a CP-odd eigenstate. The ratio of rates for $J/\psi f_0(980)$ to $J/\psi\phi$, with $f_0(980) \to \pi^+\pi^-$ in a ± 90 MeV mass window around the $f_0(980)$ and $\phi \to K^+K^-$ is $R^{f_0}_{\rm effective} = (21.7 \pm 1.1 \pm 0.7)\%$. Other structures at higher mass are shown to contain D-wave. The K^+K^- spectrum besides a large ϕ component has significant $f_2'(1525)$. The ratio of rates for $J/\psi f_2'(1525)$ to $J/\psi\phi$, with $f_2'(1525) \to K^+K^-$ in a ± 125 MeV mass window around the $f_2'(1525)$ is $R^{f_2'}_{\rm effective} = (19.4 \pm 1.8 \pm 1.1)\%$. These new channels may be useful for different aspects of CP violation measurements.

[1]Conference report prepared for International Europhysics Conference on High Energy Physics, Grenoble, France July 21-27, 2011; contact author: Sheldon Stone

1 Introduction

An important goal of heavy flavour experiments is to measure the CP violation phase in $\overline{B}{}^0_s$ mixing, $-2\beta_s$, which is predicted to be very small in the Standard Model (SM). A fit to current data predicts -0.037 [1]. This phase can be drastically increased by the presence of new particles beyond the SM. Thus, measuring $-2\beta_s$ is an important probe of new physics.

Constraints on β_s have been obtained by the CDF and D0 experiments at the Tevatron using the $\overline{B}{}^0_s \to J/\psi\phi$ decay mode [2]. First results from LHCb have also appeared [3]. Since the final state consists of two spin-1 particles, it is not a CP-eigenstate, yet it is well known that CP violating phases can be measured using angular analyses [4]. However, this requires more events to gain similar sensitivities than those obtained if the decay proceeds via only CP even or CP odd channels.

It was claimed by Stone and Zhang [5] that in the case of $J/\psi\phi$ the analysis is complicated by the presence of an S-wave K^+K^- system interfering with the ϕ that must be taken into account, and that this S-wave would also manifest itself by the appearance of $f_0(980) \to \pi^+\pi^-$ decays with a predicted rate

$$R_{f_0/\phi} \equiv \frac{\Gamma(B^0_s \to J/\psi f_0,\ f_0 \to \pi^+\pi^-)}{\Gamma(B^0_s \to J/\psi\phi,\ \phi \to K^+K^-)} \approx 20\%, \tag{1}$$

that is in good agreement with LHCb's first observation of these decays [6] and subsequent confirmations [7]. Here we update the previous LHCb analysis with approximately 4 times more data and with an extended $\pi^+\pi^-$ mass range. The mode $J/\psi K^+K^-$ is also studied since the final states opposite to the J/ψ can be populated by both $\pi^+\pi^-$ and K^+K^- and this information can be correlated. We investigate here which portions of these final states are useful for measuring β_s. The decay diagram for these processes are shown in Fig. 1.

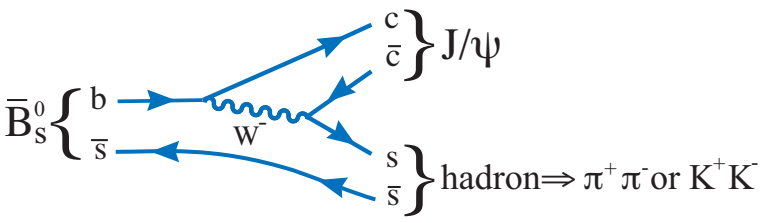

Figure 1: Leading order diagram for $\overline{B}{}^0_s$ meson decay into J/ψ and $\pi^+\pi^-$ or K^+K^- pairs.

It is important to realize that the $s\overline{s}$ system, shown in Fig. 1 is an isospin singlet (isoscalar), and thus cannot produce a single meson that is anything but $I = 0$, in the absence of higher order diagrams. All isoscalar resonances that decay strongly into $\pi^+\pi^-$ are G parity even and therefore since $G = (-1)^{L+I}$, the inherent orbital angular momentum, L, of the parent meson will be even. In fact we really only need to concern

ourselves with spin-0 and spin-2 objects as there are no known spin-4 particles in the kinematically accessible mass range below 1600 MeV. The particles that could appear are the already seen spin-0 $f_0(980)$, the spin-2 $f_2(1270)$, the spin-0 $f_0(1370)$ and the spin-0 $f_0(1500)$. The spin-2 $f_2'(1525)$ has a small branching fraction into two pions, but a large one into two kaons. The $f_2(1270)$ and the $f_0(1500)$ on the other hand have large rates into two pions and a small rates into two kaons.

2 Data sample and analysis requirements

We use a data sample of approximately 37 pb^{-1} collected with the LHCb detector in 2010 and an additional 125 pb^{-1} collected in 2011 at a center-of-mass energy of 7 TeV [8]. The detector elements are placed along the beam line of the LHC starting with the Vertex Locator (VELO), a silicon strip device that surrounds the proton-proton interaction region and is positioned 8 mm from the beam during collisions. It provides precise locations for primary pp interaction vertices, the locations of decays of long-lived particles, and contributes to the measurement of track momenta. Other devices used to measure track momenta comprise a large area silicon strip detector (TT) located in front of a 3.7 Tm dipole magnet, and a combination of silicon strip detectors (IT) and straw drift chambers (OT) placed behind. Two Ring Imaging Cherenkov (RICH) detectors are used to identify charged hadrons. Further downstream an Electromagnetic Calorimeter (ECAL) is used for photon detection and electron identification, followed by a Hadron Calorimeter (HCAL), and a system consisting of alternating layers of iron and chambers (MWPC and triple-GEM) that distinguishes muons from hadrons (MUON). The ECAL, MUON, and HCAL provide the capability of first-level hardware triggering.

This analysis is restricted to events accepted by a $J/\psi \to \mu^+\mu^-$ trigger. Subsequent analysis selection criteria are applied that serve to reject background, yet preserve high efficiencies on both the $J/\psi\pi^+\pi^-$ and $J/\psi K^+K^-$ final states, as determined by Monte Carlo events generated using PYTHIA [9], and LHCb detector simulation based on GEANT4 [10]. Tracks are reconstructed as described in Ref. [8]. To be considered as a $J/\psi \to \mu^+\mu^-$ candidate opposite sign tracks are required to have transverse momentum, $p_{\rm T}$, greater than 500 MeV, be identified as muons, and form a common vertex with fit χ^2 per number of degrees of freedom (ndof) less than 11. Di-muon candidates with masses between -48 and $+43$ MeV of the J/ψ peak are selected for further analysis.

Pion and kaon candidates are selected if they are inconsistent with having been produced at the closest primary vertex. The impact parameter (IP) is the minimum distance of approach of the track with respect to the primary vertex. We require that the χ^2 formed by using the hypothesis that the IP is equal to zero be > 9 for each track. For further consideration these tracks must be positively identified in the RICH system. Particles forming opposite-sign di-hadron candidates must have their scalar sum $p_{\rm T} > 900$ MeV.

To select B_s^0 candidates we further require that the two pions or kaons form a vertex with a $\chi^2 < 10$, that they form a candidate B_s^0 vertex with the J/ψ where the vertex fit $\chi^2/{\rm ndof} < 5$, and that this B_s^0 candidate points to the primary vertex at an angle not

different from its momentum direction by more than 0.68°, with the impact parameter χ^2 of the $\overline{B}{}^0_s$ less than 25. In addition, the $\overline{B}{}^0_s$ candidate must be inconsistent with decaying near the primary vertex with a flight distance larger than 1.5 mm.

3 Reconstruction of $\overline{B}{}^0_s \to J/\psi\pi^+\pi^-$

3.1 $\overline{B}{}^0_s \to J/\psi\pi^+\pi^-$ signal extraction

The invariant $J/\psi\pi^+\pi^-$ mass is shown in Fig. 2 for both right sign and like sign di-pion combinations. Here like sign refers to the sum of $\pi^+\pi^+$ and $\pi^-\pi^-$. From left to right we have a wide peak from misidentified $\overline{B}{}^0 \to J/\psi\overline{K}{}^{*0}$ events, a narrower peak from correctly identified $\overline{B}{}^0 \to J/\psi\pi^+\pi^-$ events, our putative $\overline{B}{}^0_s \to J/\psi f_0$ signal, and finally a broad background. The wrong-sign di-pion yield correctly describes the shape and level of the background underneath the $\overline{B}{}^0_s$ signal peak. This is consistent with our simulation which predicts that the background under the $\overline{B}{}^0_s$ signal and at higher masses is well described by the wrong-sign data.

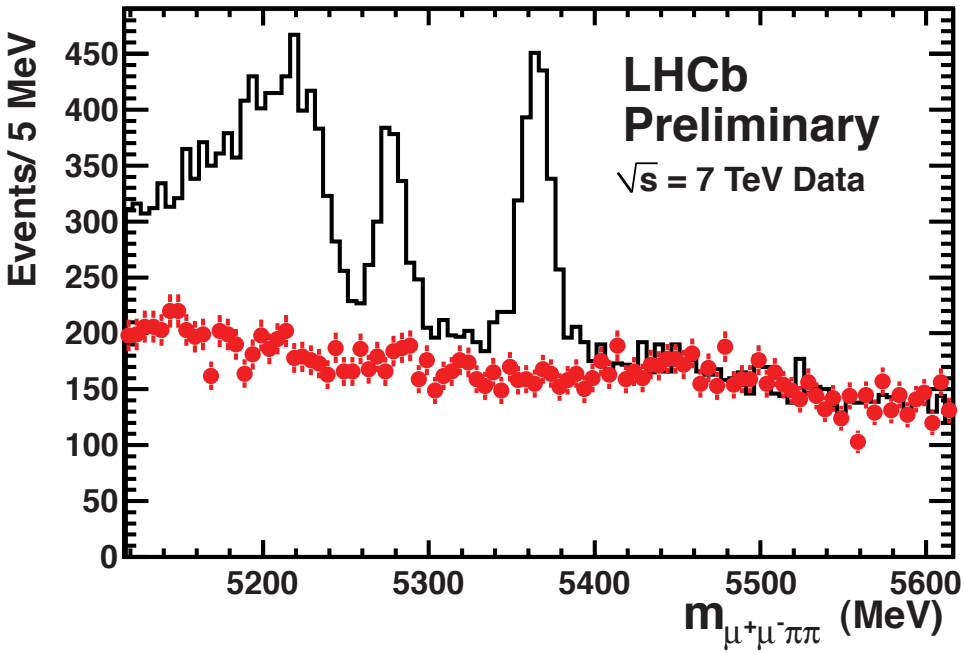

Figure 2: The invariant mass of $J/\psi\pi^+\pi^-$ combinations (histogram) and $J/\psi(\pi^+\pi^+ + \pi^-\pi^-)$ (points).

Restricting the $\pi^+\pi^-$ mass interval to be within ± 90 MeV of the $f_0(980)$ mass we again show the the B_s candidate invariant mass distribution for $J/\psi\pi^+\pi^-$ selected mass combinations in Fig. 3. The signal is fit with a Gaussian whose mean and width are allowed to float. Other components in the fit are combinatoric background taken to

have an exponential shape, $B^+ \to J/\psi K^+(\pi^+)$, $B_s \to J/\psi\eta'$, $\eta' \to \rho\gamma$, $B_s \to J/\psi\phi$, $\phi \to \pi^+\pi^-\pi^0$, and $\overline{B}^0 \to J/\psi\overline{K}^{*0}$ backgrounds. The $B^0 \to J/\psi\pi^+\pi^-$ shape is also taken to be Gaussian. The shapes of the other components are taken from Monte Carlo simulation with their normalizations allowed to float. We performed a simultaneous fit to the right-sign and wrong-sign event distributions. There are 612±30 signal events in the plot. The fit gives a B_s mass of 5366.0±0.5 MeV, in good agreement with the known

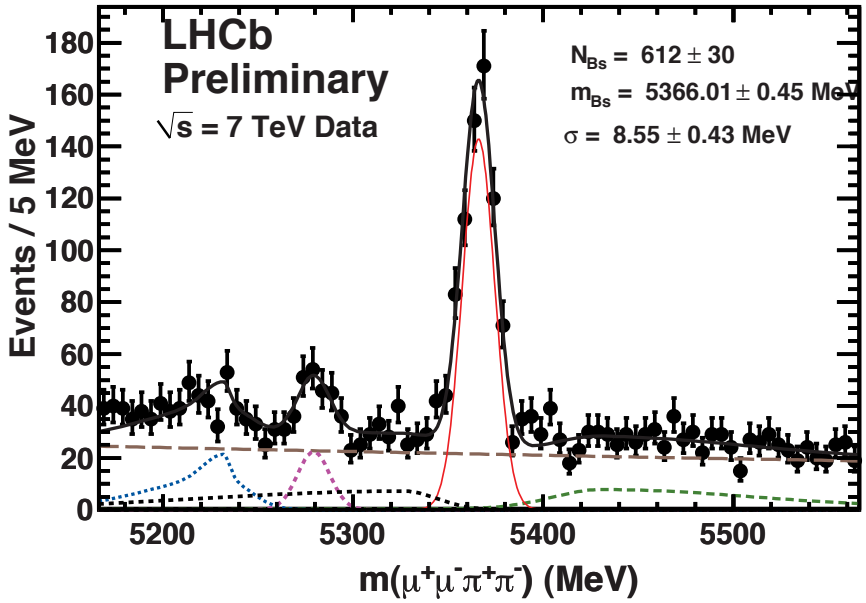

Figure 3: The invariant mass of $J/\psi\pi^+\pi^-$ combinations when the $\pi^+\pi^-$ pair is required to be with ±90 MeV of the $f_0(980)$ mass. The data have been fit with a signal Gaussian and several background functions. The thin (red) solid line shows the signal, the long-dashed (brown) line the combinatoric background, the dashed (green) line the B^+ background, the dotted (blue) line the $\overline{B}^0 \to J/\psi\overline{K}^{*0}$ background, the dash-dot line (purple) the $B^0 \to J/\psi\pi^+\pi^-$ background, the very small in level dotted line (black) the sum of $B_s \to J/\psi\eta'$ and $J/\psi\phi$ backgrounds, and the thick-solid (black) line the total.

mass of 5366.3±0.6 MeV, and a width (σ) of 8.6±0.4 MeV consistent with that previously obtained.

3.2 Study of the $\pi^+\pi^-$ mass spectrum

The Dalitz plot of the $J/\psi\pi^+\pi^-$ final state is shown in Fig. 4 for $\overline{B}_s^0$ candidate decays within ±25 MeV of the $\overline{B}_s^0$ mass. The plot includes both signal and background. The only obvious structures are in $\pi^+\pi^-$ mass with no structures visible in $J/\psi\pi^+$ mass. Next we view the $\pi^+\pi^-$ mass spectrum shown in Fig. 5. This distribution peaks at the $f_0(980)$ mass, has no significant signal below the f_0 peak, but has an excess at higher masses up to about 1550 MeV. Other known isoscalar resonances in this mass region besides the

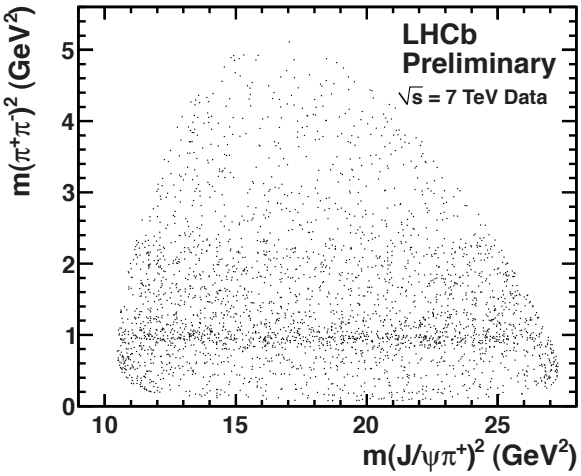

Figure 4: The invariant mass squared of $\pi^+\pi^-$ versus $J/\psi\pi^+$ for $\overline{B}{}^0_s$ candidate decays within ± 25 MeV of the $\overline{B}{}^0_s$ mass.

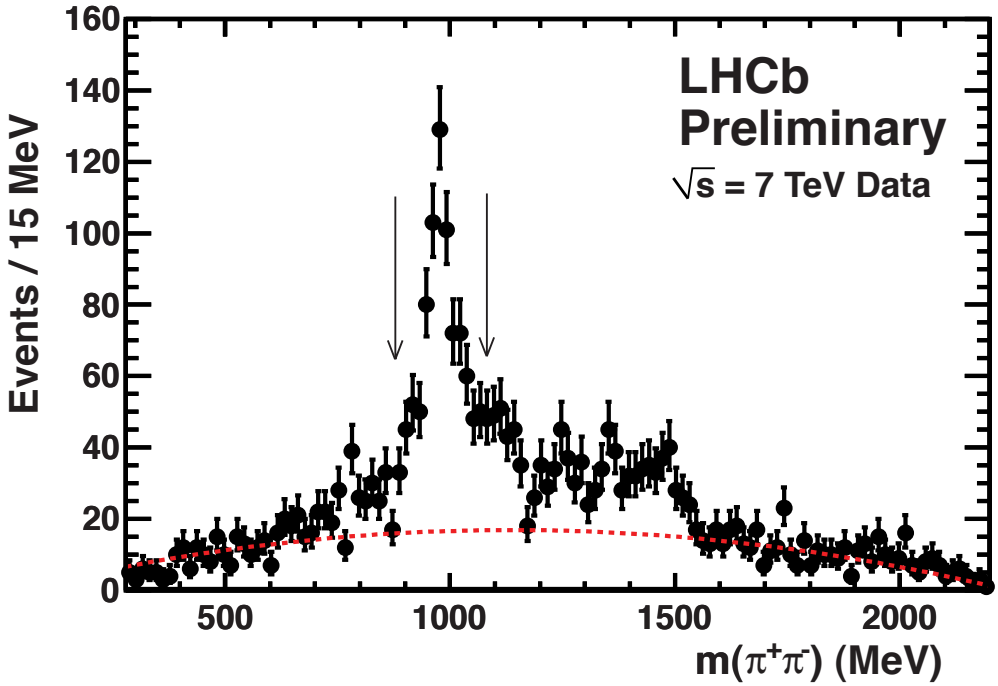

Figure 5: The invariant mass of $\pi\pi$ combinations when the $J/\psi\pi^+\pi^-$ is required to be with ± 25 MeV of the $\overline{B}{}^0_s$ mass. The data points are from $\pi^+\pi^-$ combinations and the dashed line from the sum of $\pi^+\pi^+$ and $\pi^-\pi^-$ pairs. The arrows indicate the region selected ± 90 MeV around the $f_0(980)$ peak.

$f_0(980)$ are the $f_2(1270)$, $f_0(1370)$, and $f_0(1500)$ states. While the $f_2(1270)$ mass and

width are rather well measured at 1275.1±1.2 MeV and $185.1^{+2.9}_{-2.1}$ MeV, respectively, the $f_0(1370)$ has a PDG quoted mass of 1200-1500 MeV and a width of 200-500 MeV. The $f_0(1500)$ is also relatively well measured with a mass of 1505±6 MeV and width of 109±7 MeV.

To ascertain the efficacy of using these events to measure β_s it is necessary to determine the spin-parity of the $\pi^+\pi^-$ system as a function of $\pi^+\pi^-$ mass, which requires angular analyses. To investigate the angular structure with these relatively small statistics we divide the $\pi^+\pi^-$ mass interval into two pieces, the first in the $f_0(980)$ region defined within ±90 MeV from 980 MeV; note that the full width of the $f_0(980)$ is approximately 90 MeV, but the shape is complicated as the KK threshold opens near the resonance peak [11]. The second mass interval is defined somewhat arbitrarily to be between 1200 and 1600 MeV.

For this analysis we describe the angular distributions by the coherent combination of spin-0 and spin-2 resonant decays. We use the helicity basis and define the decay angles as (1) the angle of the μ^+ in the J/ψ rest frame with respect to the $\overline{B}^0_s$ direction, $\theta_{J/\psi}$, (2) the angle of the π^+ in the $\pi^+\pi^-$ rest frame with respect to the $\overline{B}^0_s$ direction, θ_f. The spin-0 amplitude is labeled as A_{00}, the three spin-2 amplitudes as A_{2i}, $i = -1, 0, 1$, and ϕ is the strong phase between the A_{20} and A_{00} amplitudes.

After integrating over the angle between the two decay planes the joint angular distribution is given by

$$\begin{aligned}\frac{d\Gamma}{d\cos\theta_f d\cos\theta_{J/\psi}} &= \left|A_{00} + \frac{1}{2}A_{20}e^{i\phi}\sqrt{5}\left(3\cos^2\theta_f - 1\right)\right|^2 \sin^2\theta_{J/\psi} \\ &\quad + \frac{1}{4}\left(|A_{21}|^2 + |A_{2-1}|^2\right)\left(15\sin^2\theta_f\cos^2\theta_f\right)\left(1+\cos^2\theta_{J/\psi}\right). \quad (2)\end{aligned}$$

Since the $\overline{B}^0_s$ is spinless, when it decays into a spin-1 J/ψ and a spin-0 f_0, $\theta_{J/\psi}$ should be distributed as $1-\cos^2\theta_{J/\psi}$ and $\cos\theta_f$ should be flat. First we analyze the $f_0(980)$ region. The wrong-sign background subtracted, acceptance corrected helicity distributions of the data, with reconstructed $\overline{B}^0_s$ mass within ±25 MeV of the known $\overline{B}^0_s$ mass and within ±90 MeV of the $f_0(980)$ mass, are shown in Fig. 6.

We perform a joint fit to the two angular distributions and use the wrong-sign events to describe the background both in shape and normalization. The ratio of rates is

$$\begin{aligned}\frac{\Gamma_{20}}{\Gamma_{00}} &= (0.3 \pm 3.1)\% \\ \frac{\Gamma_{21}+\Gamma_{2-1}}{\Gamma_{00}} &= (2.7 \pm 4.1)\%, \quad (3)\end{aligned}$$

where Γ_{ij} indicates the square of the A_{ij} amplitude. The spin-2 amplitudes are consistent with zero. The joint fit has a χ^2/ndof of 199/196, which has a 42% probability, while fitting to only pure S-wave gives a χ^2/ndof of 204/199, a 40% probability. The fits are plotted on the figure along with the expectation for a spin-0 object. They are virtually identical for $\cos\theta_{J/\psi}$. For $\cos\theta_{f_0}$ however, there is some difference. The one-dimensional

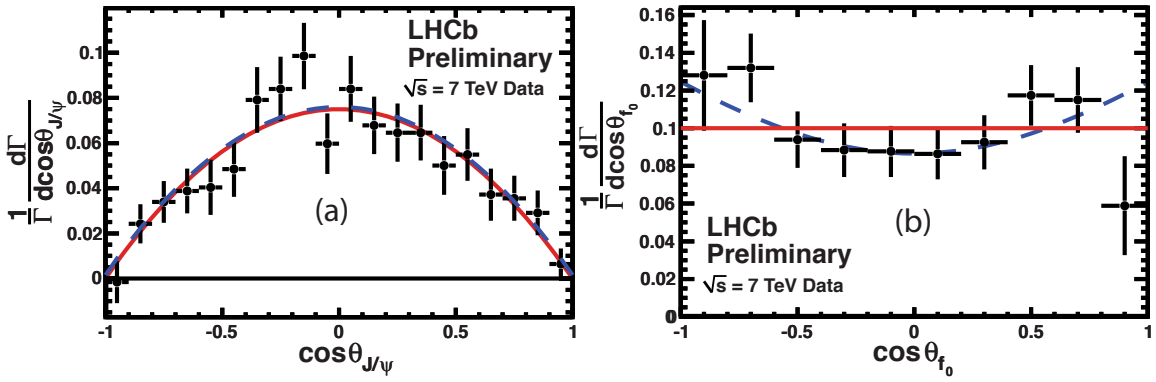

Figure 6: Efficiency corrected, background subtracted angular distributions for the $\pi^+\pi^-$ mass region within 90 MeV of 980 MeV. The dashed lines show the best fit values using the function defined in Eq. 2 and the solid lines the expectations for a spin-0 object. (a) The cosine of the angle of the μ^+ with respect to the $\overline{B}{}^0_s$ direction in the J/ψ rest frame for $\overline{B}{}^0_s \to J/\psi\pi^+\pi^-$ decays. (b) The cosine of the angle of the π^+ with respect to the $\overline{B}{}^0_s$ direction in the di-pion rest frame for $\overline{B}{}^0_s \to J/\psi\pi^+\pi^-$ decays.

χ^2 of the fit here is 9.1 for 6 degrees of freedom (17% probability) and for a flat line is 11.3 for 9 degrees of freedom (26% probability), so there really is no significant preference for one over the other.

Next we turn to the higher mass interval between 1200-1600 MeV. There are 453±28 signal events in this region. The efficiency corrected decay angular distributions are shown in Fig. 7.

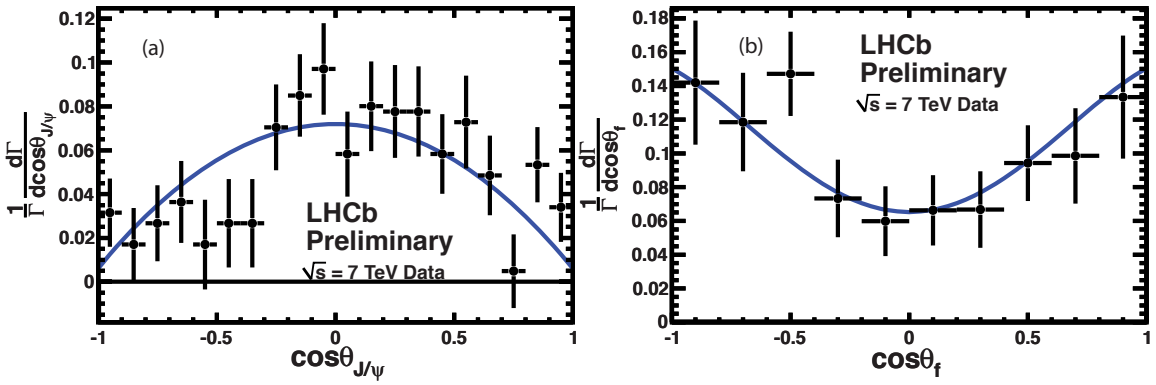

Figure 7: Efficiency corrected background subtracted angular distributions for the $\pi^+\pi^-$ mass region between 1200-1600 MeV. (a) The cosine of the angle of the μ^+ with respect to the $\overline{B}{}^0_s$ direction in the J/ψ rest frame for $\overline{B}{}^0_s \to J/\psi\pi^+\pi^-$ decays. (b) The cosine of the angle of the π^+ with respect to the $\overline{B}{}^0_s$ direction in the di-pion rest frame for $\overline{B}{}^0_s \to J/\psi\pi^+\pi^-$ decays. The curve represents a simultaneous fit performed with the function defined in Eq. 2.

Here the resulting width ratios are

$$\begin{aligned} \frac{\Gamma_{20}}{\Gamma_{00}} &= (8.1^{+15.4}_{-\ 7.3})\% \\ \frac{\Gamma_{21}+\Gamma_{2-1}}{\Gamma_{00}} &= (34.7^{+19.2}_{-13.1})\%. \end{aligned} \tag{4}$$

The phase difference ϕ is 1.15±0.44 rad. The joint fit prefers to have a significant D-wave component.

4 Analysis of $\overline{B}{}^0_s \to J/\psi K^+K^-$

4.1 $J/\psi\phi$

For di-kaon final states two types of kaon identification are used. One dubbed "loose" seeks to keep the kaon efficiency high while rejecting some pions, and the one called "tight" rejects a significantly larger fraction of pions and also eliminates protons. The relative efficiency of tight versus loose identification on two kaons is approximately 60%, with a significant enhancement, as will be shown in background rejection. This mode is used as a baseline for branching fraction measurements, thus we provide the yields here. The $J/\psi K^+K^-$ invariant mass plot for K^+K^- pairs with an invariant mass within ±20 MeV of the ϕ mass is shown in Fig. 8 (left) using loose kaon identification criteria. The data are fit with a Gaussian signal function and a linear background. The Gaussian fit gives a width (σ) of 7.21±0.11 MeV, and a yield of 2924±55 events. The expected width from Monte Carlo simulation is 5.76±0.06 MeV. For tight criteria, Fig. 8 (right), we have consistent mass and width values and 1773±42 events. For most of the subsequent analysis tight kaon identification will be used.

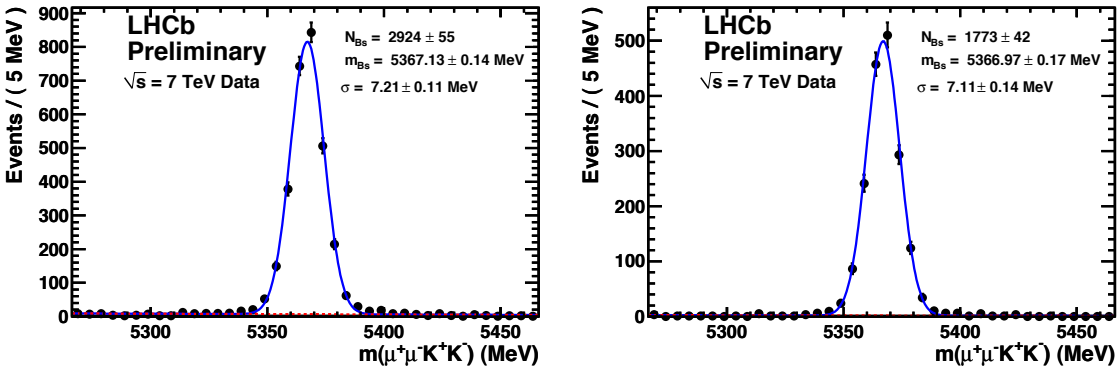

Figure 8: The invariant mass of $J/\psi K^+K^-$ combinations when K^+K^- pair is required to be with ±20 MeV of the ϕ mass (left) for loose kaon identification selection and (right) for tight selection. The data have been fit with a signal Gaussian and linear background function shown as a dashed line. The solid curve shows the sum.

4.2 Analysis of higher mass K^+K^-

Since the $\pi^+\pi^-$ mass region above the $f_0(980)$ is fraught with a great deal of activity, we look at the entire K^+K^- mass region for structures. The corresponding $\overline{B}{}^0_s$ candidate mass plot is shown in Fig. 9.

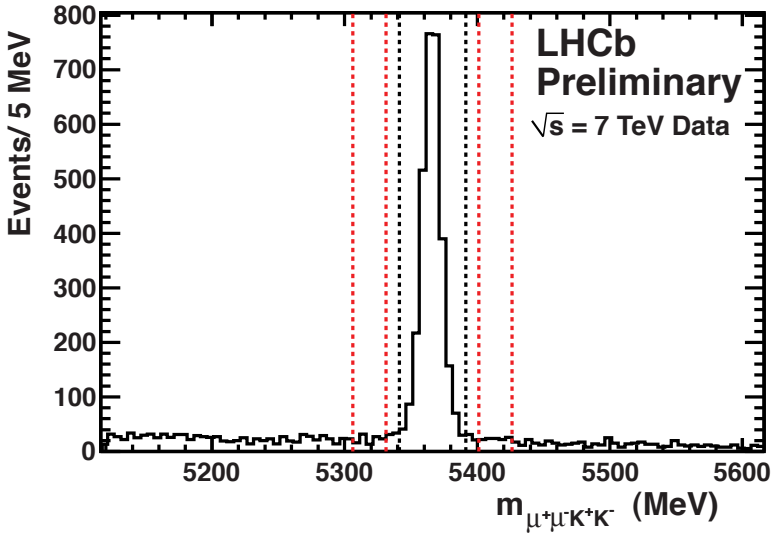

Figure 9: The invariant mass of $J/\psi K^+K^-$ combinations for the entire allowed K^+K^- mass range. The vertical lines indicate the signal and sideband regions used for subsequent analyses.

Fig. 10 shows the K^+K^- invariant mass for both signal and sideband regions, where the signal region extends ± 25 MeV around the peak and the sidebands extend from 35 MeV to 60 MeV on either side of the peak. The Dalitz plot of the $J/\psi K^+K^-$ final state is shown in Fig. 11. The plot includes both signal and background. The only obvious structures are in K^+K^- mass with nothing visible in $J/\psi K^+$ mass.

There are two new interesting features visible in this plot.

1. There is a Breit-Wigner shaped peak near 1525 MeV, the mass of a known f_2' resonance.

2. There is an excess of signal events over sidebands over most of the mass range.

4.2.1 $\overline{B}{}^0_s \to J/\psi f_2'(1525)$

Knowledge of the properties of the $f_2'(1525)$ as listed in the PDG are a mass of 1525 ± 5 MeV and a width of 73^{+6}_{-5} MeV [12]. The PDG, when referring to both the mass and width states, however: "This is only an educated guess; the error given is larger than the error on the average of the published values." Indeed examination of the measurements shows a wide spread in values.

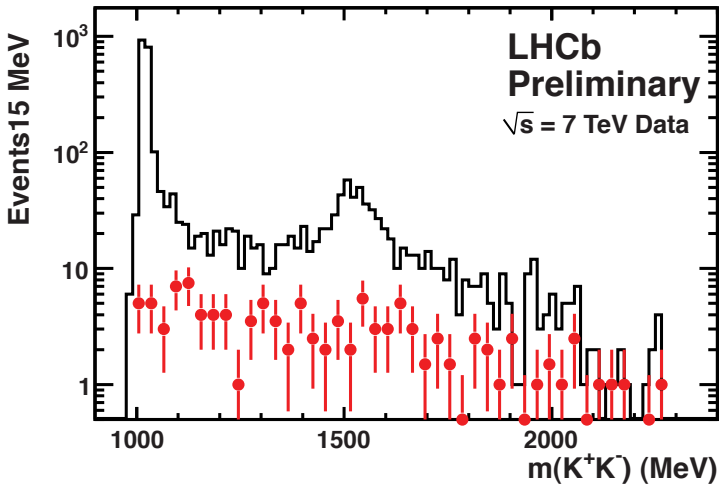

Figure 10: The invariant mass of K^+K^- combinations when the $J/\psi K^+K^-$ mass is required to be with ± 25 MeV of the B_s mass. The histogram shows the data in the signal region while the points (red) show the sidebands.

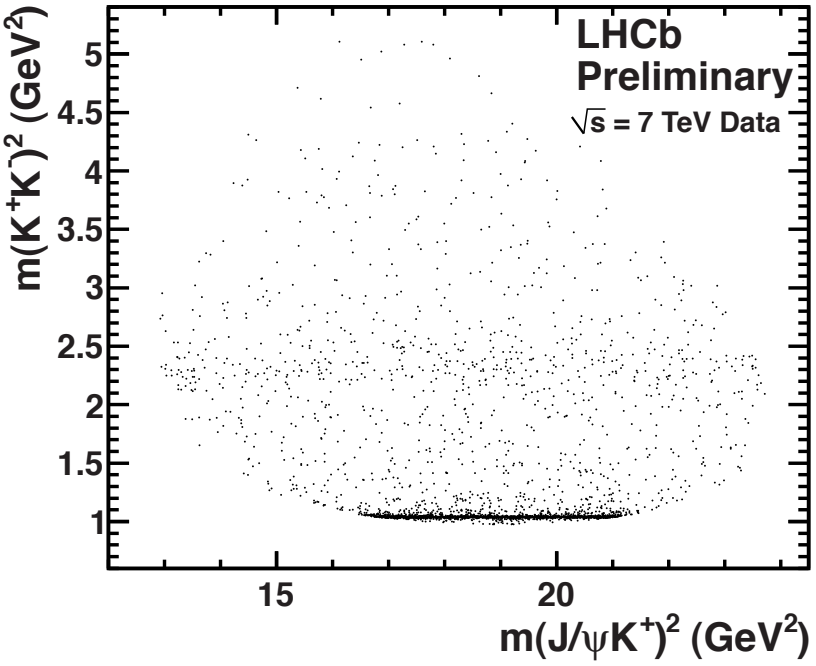

Figure 11: The invariant mass squared of K^+K^- versus $J/\psi K^+$ for $\overline{B}{}^0_s$ candidate decays within ± 25 MeV of the $\overline{B}{}^0_s$ mass.

Since this is a new $\overline{B}{}^0_s$ decay mode we are concerned about checking that part or all of the signal may be from other B to J/ψ exclusive decay modes. An examination of the

Particle Data Book reveals no exclusive final states that have been observed in $\overline{B}^0$ decays to $J/\psi K^-\pi^+$ decay modes that might reflect into a $\overline{B}_s^0$ state near 1525 MeV in K^+K^- mass if the pion is misidentified as a kaon [12]. We did notice, however, that the BaBar Collaboration observes a $K^-\pi^+$ mass peak in $\overline{B}^0 \to J/\psi K^-\pi^+$ decays at a mass close to that of the known $\overline{K}_2^*(1430)$ resonance [13]. To ensure that we are not being subject to a reflection in the 1525 MeV di-kaon mass region, a simulation of $\overline{B}^0 \to J/\psi \overline{K}_2^*(1430)$ decays was performed where the π^+ from the $\overline{K}_2^*(1430)$ was interpreted as a K^+.[2] No attempt was made to predict an absolute rate based on the π to K misidentification rate, and the relative rate of B^0/B_s production [14], because of the unmeasured branching ratio. Fig 12 shows the shape of this reflection in $\overline{B}_s^0$ and di-kaon mass.

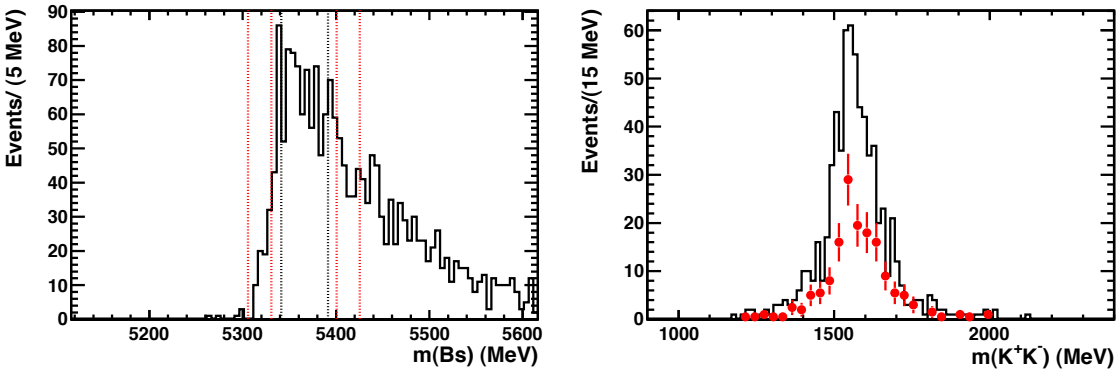

Figure 12: Simulation of $\overline{B}^0 \to J/\psi \overline{K}_2^*(1430)$ decays where the π^+ from the $\overline{K}_2^*(1430)$ decay is interpreted as a K^+. (Left) the $\overline{B}_s^0$ invariant mass, where the vertical lines show the signal and sideband regions, and (right) $m(K^+K^-)$ where the histogram shows events in the signal region of $\overline{B}_s^0$ mass and the points show those in the sideband region.

Evidently we can be victims of a reflection here and the sideband subtraction does not subtract off enough events to remove the effect. Thus we need to ascertain the size of this effect. To measure the size of any $\overline{B}^0$ reflection in the $f_2'(1525)$ mass region, within ± 300 MeV of 1525 MeV, we reassign each kaon in turn to the pion hypothesis and plot the $J/\psi K\pi$ mass, when the reconstructed $\overline{B}_s^0$ mass is in the range 25-200 MeV above the $\overline{B}_s^0$ mass. The data are shown in Fig. 13. The resulting peak has 35.5 ± 9.8 events for tight kaon identification cuts, a 94% reduction from that using loose cuts.

To ascertain the number of $f_2'(1525)$ events we perform a simultaneous fit to the $\overline{B}_s^0$ candidate mass and the di-kaon mass. The $f_2'(1525)$ signal is parameterized by a spin-2 Breit-Wigner function [15]. PDF's are included for non-resonant K^+K^-, a straight line, as well as $\overline{K}^*$ reflected backgrounds, where the normalization is fixed from the fit yield of 35.5 ± 9.8 events shown in Fig. 13 extrapolated using the simulated shape into the $\overline{B}_s^0$ fit region. The width of the $f_2'(1525)$ is constrained to the PDG value of 73 MeV [12].

[2]Here and wherever appropriate, charge conjugate modes are also considered.

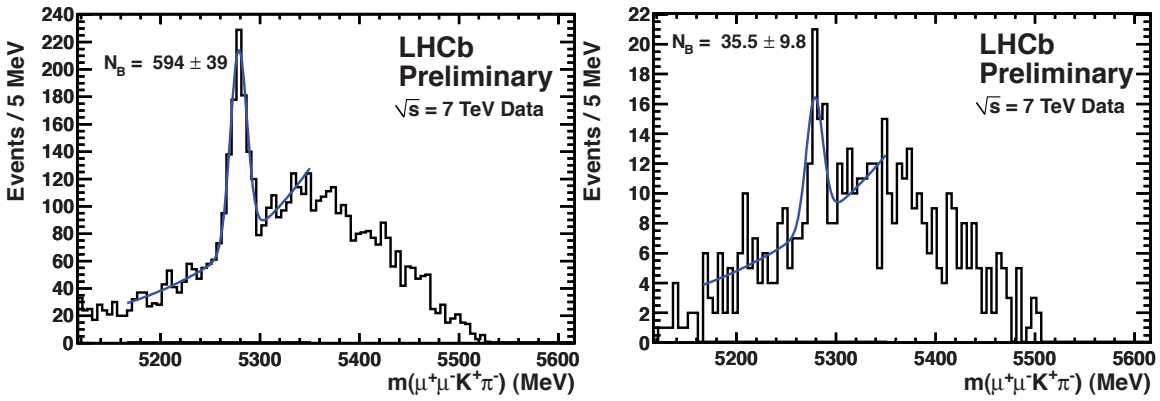

Figure 13: $\overline{B}{}^0_s \to J/\psi K^+K^-$ candidates 25-200 MeV above the $\overline{B}{}^0_s$ mass and with $m(K^+K^-)$ within 300 MeV of 1525 MeV, reinterpreted as $J/\psi K\pi$ events. The fit is to a signal Gaussian whose mass and width are allowed to float. (Left) loose kaon ID criteria, and (right) tight kaon ID criteria.

The results of the fits are shown in Fig. 14. The resulting mass from the fit is 1525±4 MeV and there are 296±26 events. If we allow the width to float we find a consistent value of 90^{+16}_{-14} MeV. As we have not taken into account possible interferences between the

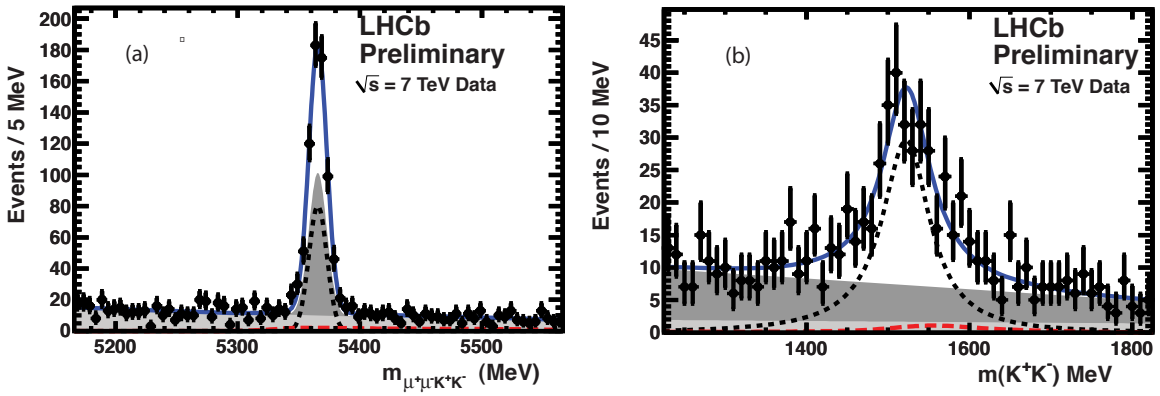

Figure 14: Projections of fits to the $\overline{B}{}^0_s$ candidate mass and the di-kaon mass. The $f_2'(1525)$ signal is parameterized by a spin-2 Breit-Wigner function. The combinatoric background is shown in the light shaded region, while the darker shaded region shows the non-resonant $J/\psi K^+K^-$ component. The width is fixed to the PDG value of 73 MeV. The long-dashed (red) line shows the $\overline{B}{}^0 \to J/\psi K^-\pi^+$ decays.

$f_2'(1525)$ and other $J/\psi K^+K^-$ final states we do not quote measured values of the mass and width at this time.

The $f_2'(1525)$ is a G-parity even state and its spin has been measured as two [12]. Shown in Fig. 15 is the background subtracted, acceptance corrected helicity distribution of the J/ψ for K^+K^- masses in the f_2' region. The points are extracted in $\cos\theta_{J/\psi}$ from

the joint fit to the $\overline{B}_s^0$ candidate decays and $m(K^+K^-)$ in the K^+K^- mass region within 1400-1650 MeV for events in the peak above the non-resonant K^+K^-. The sidebands in $\overline{B}_s^0$ mass are used to subtract the background. The data are fit to a functional form resulting from integrating Eq. 2 over $\cos\theta_f$

$$f(\cos\theta_{J/\psi}) = (1-p)\sin^2\theta_{J/\psi} + \frac{p}{2}\left(1+\cos^2\theta_{J/\psi}\right), \tag{5}$$

where $1-p$ is the fraction of helicity zero and p is the fraction of helicity 1. The fit result is $p = (51 \pm 8)\%$, with χ^2/ndof of 11.7/8 (17% probability), showing that the data are consistent with spin-2 and not consistent with pure spin-0, confirming that we are seeing the $f_2'(1525)$.

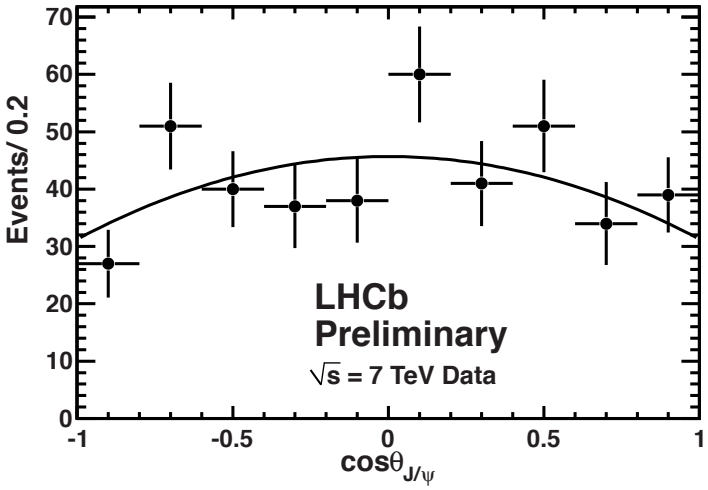

Figure 15: The cosine of the angle of the μ^+ with respect to the $\overline{B}_s^0$ direction in the J/ψ rest frame for $\overline{B}_s^0 \to J/\psi f_2'(1525)$ decays. The background and non-resonant K^+K^- components have been removed. The data are fit to the function described in the text. Note that for pure S-wave such as $J/\psi f_0$ the distribution would be $\sin^2\theta_{J/\psi}$.

5 Relative yields of $J/\psi f_0(980)$, and $J/\psi f_2'(1525)$ to $J/\psi\phi$ events

To establish a value for the ratio of $f_0(980)$ to $J/\psi\phi$ branching fractions requires fitting the $\pi^+\pi^-$ mass spectrum with a realistic shape for the $f_0(980)$. We leave for another day a full analysis of this final state as a function of $\pi^+\pi^-$ mass. We will only update our value for $R^{f_0}_{\rm effective}$, defined as the ratio of the number of $J/\psi\pi^+\pi^-$ events within ± 90 MeV of the f_0 mass, 980 MeV, and the number of $J/\psi K^+K^-$ events within ± 20 MeV of the ϕ mass; effectively these are the event yields that will be used to measure β_s. In

our ±90 MeV interval about 980 MeV we find 612±30 signal events above background. Using looser kaon identification criteria we find 2924±55 $J/\psi\phi$ events. Table 1 shows the efficiencies for detecting the various final states. Note that only the relative efficiencies matter, and most errors cancel in this ratio. The pion and kaon efficiencies are corrected with respect to those given in the Monte Carlo simulation by using D^{*+} and K_S samples where the pions and kaons are selected without resorting to the PID information. Briefly, we measure the efficiency with respect to Monte Carlo in bins of p_t and η and then weight the averages from the distributions in data. The efficiency is obtained by simultaneously fitting the invariant mass distributions of events either passing or failing the identification requirements.

After correcting for the relative efficiencies we find

$$R^{f_0}_{\rm effective} = (21.7 \pm 1.1 \pm 0.7)\%. \tag{6}$$

The systematic error will be discussed subsequently.

Table 1: Monte Carlo simulated efficiencies (%) for each J/ψ decay mode. Loose and tight refer to the kaon identification criteria. The PID correction is determined from data. The quoted uncertainties are statistical only.

Mode	Tracks within 10-400 mrad	Recon. +trigger	PID	Total	Total relative to $J/\psi\phi$ (loose)
ϕ (loose)	15.97±0.15	7.43±0.03	98.5±0.3	1.17±0.01	1
ϕ (tight)	15.97±0.15	5.28±0.03	83.6±0.4	0.70±0.01	0.60±0.01
$f_0(980)$	13.99±0.06	8.32±0.09	97.0±0.1	1.13±0.01	0.97±0.02
					Rel. to ϕ tight
$f_2'(1525)$ avg	15.26±0.06	4.13±0.09	87.4±0.5	0.551±0.012	0.781± 0.019

Our value is in good agreement with the original estimate by Stone and Zhang of 20% [5], although that prediction was for the total $f_0(980)$ yield, $R_{f_0/\phi}$, not the effective yield, which is somewhat smaller. Other theoretical estimates for $R_{f_0/\phi}$ have a rather wide range from 7-50% [16]. To find the relative rate of $f_2'(1525)$ decays, the sample with tight kaon selection is used, and the fit where the width is allowed to float. $R^{f_2'}_{\rm effective}$ is defined as the efficiency corrected ratio of the number of events in the K^+K^- mass interval between 1400 and 1650 MeV. We measure

$$R^{f_2'}_{\rm effective} = (19.4 \pm 1.8 \pm 1.1)\% \tag{7}$$

The systematic errors will be discussed subsequently.

5.1 Systematic errors

The relative kaon versus pion efficiency is known to 1% per track giving a systematic error of 2% for $f_0(980)$ relative to ϕ. An additional systematic error of 1% is added to all the

modes to account for different momentum distributions of the kaons even in final states with equal number of kaons due to different momentum distributions. As a check we note that the ratio of the number of events in $J/\psi\phi$ with tight cuts to loose cuts on the kaon identification is (61±2)% and the simulation gives a consistent (60±1)%.

The systematic errors have several contributions listed in Table 2 for the three different ratios. We include an uncertainty for a mass dependent efficiency as a function of $\pi^+\pi^-$ mass by changing the acceptance function from flat to linear and found that the f_0 yield changed by 2.3%. There is a larger effect due to the possible changes in the helicity distributions of the $f_2'(1525)$ that can be either helicity zero or helicity one. The difference between the average value using both helicities and either value is 4%, which we use for the systematic uncertainty. Changing the fixed width of the $f_2'(1525)$ by ±6 MeV, the PDG error, results in a 2.4% change in the yield. The uncertainty on the background shapes was evaluated by changing the nominal exponential background shape to a second order polynomial. The changes are on the order of 1%.

The number of $f_0(980)$ and ϕ signal events can also be evaluated using a double Gaussian signal function. In this case the ratio of events changes by 1%.

Table 2: Systematic uncertainties on the relative rates(%).

Variable	$R^{f_0}_{\rm effective}$	$R^{f_2'}_{\rm effective}$
h^+h^- mass dependent efficiency	2.3	2.3
$\overline{B}{}^0_s$ p_t distribution	0.5	0.5
$\overline{B}{}^0_s$ mass resolution	0.5	0.5
PID	2.0	1.0
$f_2'(1525)$ width	-	2.4
$f_2'(1525)$ helicity	-	4.0
Background Shape	0.7	1.3
Signal Shape	1.0	1.0
Total	3.4	5.5

6 Conclusions

Using an approximately four times larger data sample than in our discovery paper LHCb measures

$$R^{f_0}_{\rm effective} \equiv \frac{\mathcal{B}(B^0_s \to J/\psi f_0,\ f_0 \to \pi^+\pi^-)}{\mathcal{B}(B^0_s \to J/\psi\phi,\ \phi \to K^+K^-)} = (21.7 \pm 1.1 \pm 0.7)\% \quad \text{for } \left|m(\pi^+\pi^-) - 980\ \text{MeV}\right| < 90\ \text{MeV}. \tag{8}$$

The value has increased within error from our previous measurement of (16.6±2.2±1.6)%. Both new and old values are in good agreement with the original estimate by Stone and Zhang of ∼20% [5]. The theoretical predictions are summarized by Stone [17]. The events

in the f_0 peak are shown to be dominantly S-wave and thus this is a CP-odd eigenstate useful for measuring β_s.

We have made the first observation of $\overline{B}{}^0_s \to J/\psi f_2'(1525)$ decays. The effective rate is

$$R^{f_2'}_{\text{effective}} \equiv \frac{\mathcal{B}(B^0_s \to J/\psi f_2'(1525),\ f_2'(1525) \to K^+K^-)}{\mathcal{B}(B^0_s \to J/\psi\phi,\ \phi \to K^+K^-)} = (19.4 \pm 1.8 \pm 1.1)\% \quad \text{for } \left|m(K^+K^-) - 1525 \text{ MeV}\right| < 125 \text{ MeV}. \tag{9}$$

This decay mode can also be used to measure β_s although a transversity analysis would be required as in $J/\psi\phi$, and since the final state is a combination of a spin-1 J/ψ and a spin-2 f_2' the amplitudes would be different than in $J/\psi\phi$ [18]. It is also possible that this mode could be used to resolve ambiguities in β_s if the interference with non-resonant $J/\psi K^+K^-$ is significant.

References

[1] J. Charles *et al.*, Eur. Phys. J. C**41** (2005) 1 hep-ph/0406184.

[2] I. Ripp-Baudot, presented at 13th Int. Conf. on B-Physics at Hadron Machines, April 4th-8th 2011, Amsterdam, The Netherlands, http://indico.cern.ch/contributionDisplay.py?contribId=10&confId=100779, to appear in proceedings.

[3] LHCb-Conf-2011-006, http://cdsweb.cern.ch/record/1328957/files/LHCb-CONF-2011-003.pdf .

[4] I. Dunietz, H. R. Quinn, A. Snyder, W. Toki and H. J. Lipkin, Phys. Rev. D **43**, 2193 (1991); J. L. Rosner, Phys. Rev. D **42**, 3732 (1990); A. S. Dighe, I. Dunietz, H. J. Lipkin and J. L. Rosner, Phys. Lett. B **369**, 144 (1996), hep-ph/9511363.

[5] S. Stone and L. Zhang, Phys. Rev. D**79** (2009) 074024 [arXiv:0812.2832].

[6] R. Aaij *et al.* (LHCb Collaboration), Phys. Lett. **B** 698 (2011) 115 arXiv:1102.0206 [hep-ex].

[7] J. Li *et al.* (Belle Collaboration), Phys. Rev. Lett. **106** (2011) 121802 arXiv:1102.2759 [hep-ex]; T. Aaltonen *et al.*, (CDF Collaboration), arXiv:1106.3682 [hep-ex]; D0 Collaboration, D0 Note 6152-CONF http://www-d0.fnal.gov/Run2Physics/WWW/results/prelim/B/B62/B62.pdf (2011).

[8] A. Augusto Alves Jr. *et al.*, (LHCb Collab.) "The LHCb Detector at the LHC," JINST **3** S08005 (2008).

[9] T. Sjöstrand, S. Mrenna and P. Skands, "PYTHIA 6.4: Physics and manual", JHEP **05** (2006) 026.

[10] S. Agostinelli *et al.*, Nucl. Instrum. and Meth. **506** (2003) 250.

[11] S.M. Flatté, Phys. Lett. B **63** (1976) 224.

[12] K. Nakamura *et al.*. (Particle Data Group), J. Phys. G **37** (2010) 075021.

[13] B. Aubert *et al.* (BaBar Collaboration), Phys. Rev. Lett. **87** (2001) 241801; B. Aubert *et al.* (BaBar Collaboration), Phys. Rev. D (2009) 112001.

[14] LHCb-CONF-2011-028; http://cdsweb.cern.ch/record/1356181/files/LHCb-CONF-2011-028.pdf ; arXiv:1106.4435 at http://arxiv.org/pdf/1106.4435 .

[15] R. Mizuk*et al.* (Belle Collaboration), Phys. Rev. D **78** (2008) 072004.

[16] K. M. Ecklund *et al.* (CLEO), Phys. Rev. D **80** (2009) 052009. arXiv:0907.3201 [hep-ex]; P. Colangelo, F. De Fazio and W. Wang, Phys. Rev. D**81** (2010) 074001 arXiv:1002.2880 [hep-ph]; P. Colangelo, F. De Fazio and W. Wang, "Nonleptonic B_s to charmonium decays: analyses in pursuit of determining the weak phase β_s," arXiv:1009.4612 [hep-ph]; P. Colangelo, F. De Fazio, P. Santorelli and E. Scrimieri, Phys. Rev. D**53** (1996) 3672; Erratum-ibid. D**57** (1998) 3186; O. Leitner *et al.*, "Scalar resonance effects on the $B_s - \overline{B}_s$ mixing angle," arXiv:1003.5980 [hep-ph].

[17] S. Stone arXiv:1009.4939 [hep-ph].

[18] Some consideration has been given to measuring CP violation in vector-tensor decays. See C. Sharma and R. Sinha, Phys. Rev. D **73** (2006) 014016 [arXiv:hep-ph/0504178].